

RESEARCH ON PARAMETERS OF MMC FRACTURE CRITERION FOR ADVANCED HIGH STRENGTH DUAL-PHASE STEEL SHEETS

QIUTAO FU

School of Traffic and Vehicle Engineering, Shandong University of Technology, Zibo, China

DI LI

School of Transportation and Vehicle Engineering, Shandong University of Technology, Zibo, China

email: hahali@sdut.edu.cn

HUI SONG, XINGFENG LIU, ZIPENG LU, HONGJIAN CUI

School of Traffic and Vehicle Engineering, Shandong University of Technology, Zibo, China

To predict the shear fracture, tests of advanced high-strength DP steels have been carried out, and fracture models of DP steels have been established using the MMC fracture model. The MMC fracture parameters were obtained through multiple sets of experiments and stress triaxiality solved by simulation. The result was verified by stretch-bending, Nakazima tests and simulations. It shows that the MMC criterion is suitable for predicting ductile fracture of DP980, 1180. The correlation between the parameters of the MMC criterion and DP steel material properties can reduce the amount of tests data required.

Keywords: advanced high strength dual-phase steel, plasticity, shear fracture, modified Mohr-Coulomb criterion, parameter correlation

1. Introduction

Advanced high-strength steels (AHSS), especially advanced high strength dual-phase (DP) steels, have the advantages of a low yield ratio and high collision performance. It is an important material to achieve a lightweight body, so it has been widely used in the automotive industry in recent years. However, various issues have arisen during manufacturing processes of AHSS. A typical problem occurs during stamping is a ductile fracture termed the shear fracture which has no obvious necking phenomenon and almost no thinning at the fracture (Gotoh *et al.*, 1997; Sriram *et al.*, 2003; Walp *et al.*, 2006; Shih and Shi, 2008; Levy and Van Tyne, 2009; Shih *et al.*, 2008; Shih, 2009). Due to the incompetence of the forming limit diagram (FLD) for industrial applications, it cannot predict this type of shear fracture for the dual-phase steel.

A lot of study on shear fracture of a dual-phase steel sheet have launched and appeared phenomenological models that are most suitable for industrial applications. The phenomenological ductile fracture model called the “Modified Mohr-Coulomb” (MMC) model is currently more widely used (Bai and Wierzbicki, 2010) to predict shear fracture damage of a dual-phase steel sheet. Wierzbicki *et al.* (2005) compared several widely used failure criteria through experiments on aluminum alloy materials, and summarized the change law of stress triaxiality for most of the failure criteria. The calculations of Xue (2007) and Xue and Wierzbicki (2009) show that the key factors determining the shear fracture are the third invariant of the stress state and softening due to damage. The MMC criterion proposed by Bai-Wierzbicki was based on aluminum alloy materials. Later research was extended to a DP steel. The study by Li (2010) *et al.* found that the MMC criterion can be applied to stress triaxiality between -2 and 1 . Lou and Huh (2013) also adopted the MMC criterion to study the failure behavior of an advanced high-strength steel under different stress triaxial degrees. Lian *et al.* (2013, 2015) also used the MMC criterion

considering the stress triaxiality and the lode angle to study the influence of stress triaxiality on the plastic behavior and fracture phenomena by designing different three-point bending experiments. Ji *et al.* (2020) conducted tensile tests on aluminum alloy samples with different stress triaxial degrees and Rod angles, different loading directions, different strain rates, and developed an improved MMC-based fracture model to describe the relevant fracture characteristics. They combined a test and simulation to verify the reliability of the criterion. Qian *et al.* (2020) proved the superiority of the MMC fracture criterion by designing five fracture tests of advanced high-strength steel TRIP780 from the shear stress state to tensile stress state and employing scanning electron microscopy of the fracture. Granum *et al.* (2021) presented a novel calibration procedure of the modified Mohr-Coulomb (MMC) fracture model by localization analysis and applied it for AA6016 aluminium alloy, and reduced the number of mechanical tests required to calibrate the MMC fracture model in a certain extent.

To our knowledge, the fracture criterion used for numerical simulation is relatively complete. However, the applicability of the MMC fracture criterion to DP980 and DP1180 needs further study due to the complexity of deformation of the sheet metal. On the other hand, validating three parameters of the MMC fracture criterion requires multiple sets of test data as a basis, and the solution process is cumbersome. Due to three parameters of the MMC fracture criterion are relevant to material properties, if we can develop a relationship formula between three parameters of the MMC fracture criterion and material properties for an advanced high-strength dual-phase steels sheet, it is very helpful to validate these MMC parameters.

In this paper, uniaxial tensile and shear tests were performed on DP590, DP780, DP980, and DP1180, and the Hill orthotropic elasto-plastic model and the MMC fracture criterion were used to comprehensively characterize the plastic behavior and ductile fracture properties of the plates. A numerical program employing the user material subprogram of Abaqus Explicit was performed to compare the simulation with the test results. Finally, a series of parametric studies were carried out to discuss the changes of MMC parameters under different steel sheets performance parameters, and a relationship between three parameters of the MMC fracture criterion and material properties for advanced high-strength dual-phase steels sheet was developed to help validation of the three parameters of the MMC criterion.

2. Experiments

2.1. Material

A family of advanced high strength steels is comprised of a variety of steels, most of which are multiphase materials with tensile strength greater than 600 MPa, such as Dual-Phase steel (DP), Transformation Induced Plasticity steel (TRIP), etc. This paper selects DP590, DP780, DP980 and DP1180 steels produced by Shanghai Baosteel Company for research. The microstructure of DP steels mainly consists of two phases: ferrite and martensite.

2.2. Plasticity characterization

A complete plasticity model consists of the yield criterion, the flow rule and the hardening rule. In the literature, various yield criteria have been used to simulate AHSS: von Mises isotropic yield criterion (Yoshida *et al.*, 2008; Durrenberger *et al.*, 2008). Hill (1948) quadratic orthotropic yield criterion; non-quadratic anisotropic Barlat yield criterion (Barlat *et al.*, 2003; Lee *et al.*, 2005). In this paper, due to the anisotropy of the DP steel sheet, we make use of the Hill (1948) orthotropic yield criterion to build a simulation model of the DP steel sheet. The yield condition reads

$$\bar{\sigma} = \sqrt{F(\sigma_y - \sigma_z)^2 + G(\sigma_z - \sigma_x)^2 + H(\sigma_x - \sigma_y)^2 + 2L\sigma_{yz}^2 + 2M\sigma_{zx}^2 + 2N\sigma_{xy}^2} \quad (2.1)$$

where $\bar{\sigma}$ is the Hill (1948) equivalent stress, σ_i represents the component of the Cauchy stress tensor, the six constants F - N are anisotropic parameters.

The hardening law defines the method of establishing the subsequent yield surface, and its form changes with different materials. In this paper, the swift hardening law is used to fit the stress-strain curve of the uniform extension of the DP steel

$$\sigma = K(\varepsilon_0 + \bar{\varepsilon}_p)^n \tag{2.2}$$

where K is the hardening coefficient, ε_0 represents the pre-strain, n denotes the hardening index, and $\bar{\varepsilon}_p$ is the plastic strain.

By simplifying Eq. (2.3) and transforming it into a linear formula, the K and n values are initially determined by obtaining the slope and intercept of the specimen curve from the yield point to the tensile strength point. The steel plant provided performance parameters of the DP steel and determined the anisotropy parameters as shown in Table 1.

Table 1. Hill’s constants of steel sheets

Steel	F	G	H	L	M	N
DP590	0.84	1.023	0.98	2.768	2.768	2.768
DP780	0.56	0.56	0.44	1.5	1.5	1.5
DP980	0.4907	0.573	0.427	1.38	1.38	1.38
DP1180	0.46	0.55	0.45	1.46	1.46	1.46

2.3. Uniaxial tensile test

The WDW-20D material performance testing machine was used to conduct uniaxial tensile tests on DP590, DP780, DP980, and DP1180 in DP steel sheets. A single tensile test specimen was shown in Fig. 1. Engineering stress-strain curves for four types of DP steels are shown in Fig. 2. Through the data processing of the elastic and plastic section of the test stress-strain curve, the performance parameters of each steel sheet are obtained. Material properties are listed in Table 2.

Table 2. Material properties

Steel	E	u	K	n
DP590	201000	0.28	950-1000	0.175
DP780	215000	0.29	1000-1050	0.11
DP980	216000	0.29	1150-1180	0.08
DP1180	218000	0.29	1250-1360	0.06

2.4. Shear test

In order to study a series of shear fracture phenomena of AHSS, a series of shear specimens (Fig. 2) were designed to conduct shear tests with angles under different steel sheets through a testing machine. Figure 3 shows shear load-displacement curves of DP590, DP780, DP980 and DP1180 steel sheets at different shear angles.

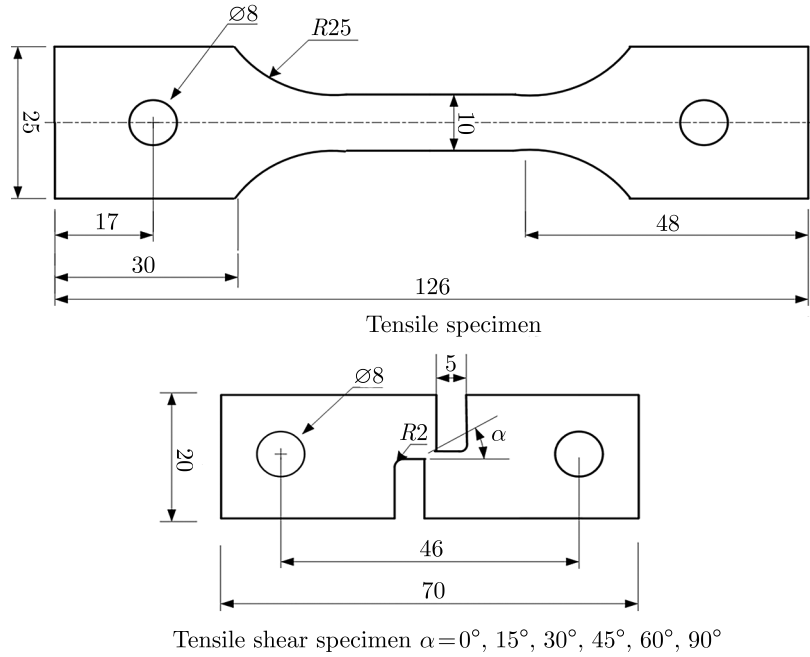


Fig. 1. Uniaxial tension test specimens

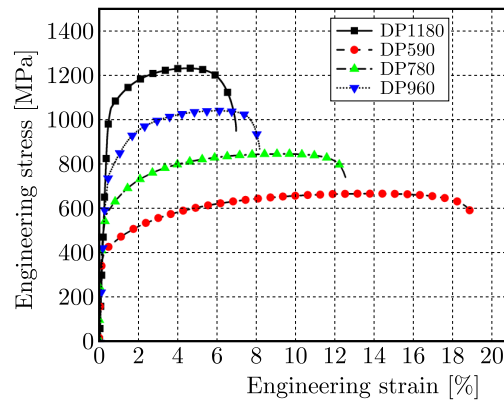


Fig. 2. Engineering stress-strain curve of dual-phase (DP) steel

3. Fracture modeling

3.1. MMC ductile fracture model

As mentioned in Section 1, Bai and Wierzbicki (2010) derived a novel functional form of the MMC fracture envelope by transforming the classical stress-based Mohr-Coulomb failure criterion into the space of stress triaxiality, Lode angle parameter and equivalent plastic strain

$$\hat{\varepsilon} = \left\{ \frac{K}{c_2} \left[c_3 + \frac{\sqrt{3}}{2 - \sqrt{3}} (1 - c_3) \left(\sec\left(\frac{\bar{\theta}\pi}{6}\right) - 1 \right) \right] \left[\sqrt{\frac{1 + c_1^2}{3}} \cos \frac{\bar{\theta}\pi}{6} + c_1 \left(\eta + \frac{1}{3} \sin \frac{\bar{\theta}\pi}{6} \right) \right] \right\}^{-\frac{1}{n}} \quad (3.1)$$

where the equivalent strain is a function based on the stress triaxiality η and the Rod angle parameter $\bar{\theta}$, A and n are Swift law hardening parameters, and C_1 , C_2 , C_3 are three material constants which should be calibrated through at least three sets of shear experiments and simulation calibration.

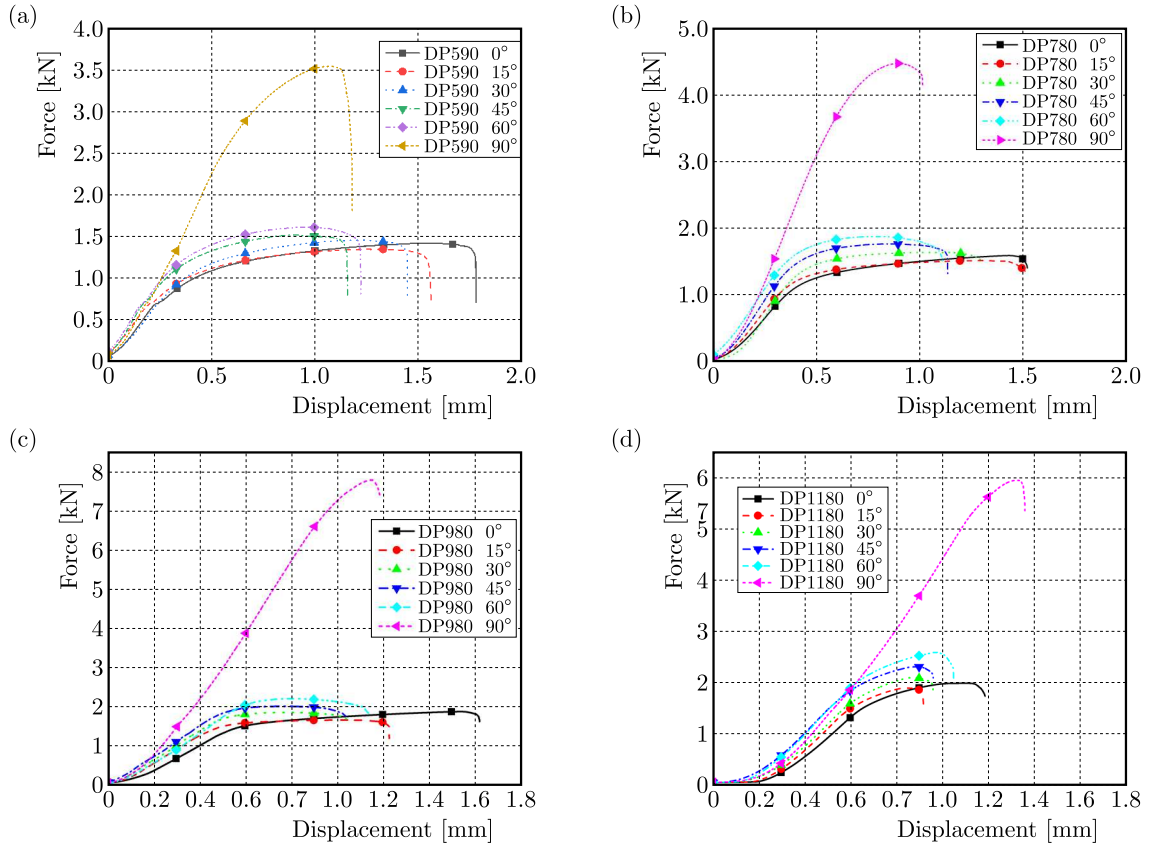


Fig. 3. Load-displacement curves of shear tests

A unique relationship between the triaxiality and Lode angle has been obtained by Wierzbicki and Xue (2005).

$$-\frac{27}{2}\eta\left(\eta^2 - \frac{1}{3}\right) = \cos(2\theta) = \sin \frac{\pi\bar{\theta}}{2} \quad \eta = \frac{\sigma_m}{\bar{\sigma}} \quad (3.2)$$

The stress triaxiality is a dimensionless parameter. The stress triaxiality is always negative in the compression state. Its value is 0 in the pure shear state, it is 1/3 in uniaxial tension, and its value is $-1/3$ in uniaxial compression. There are currently few calculation formulas that can accurately characterize the ultimate equivalent strain of the shear specimen. In this paper, shear simulation is used to obtain the stress triaxiality of the fracture specimen and the fracture strain obtained from the experiment (Fig. 3) to solve the MMC fracture criterion parameters.

3.2. Parameters calibration

With at least three different tests providing three unique combinations of the triaxiality η and the Rod angle $\bar{\theta}$, various optimization approaches could be taken to fit the fracture envelope to the experimental points and thus to obtain C_1 , C_2 and C_3 .

All the numerical simulations of the present tests in Section 2 were performed in the environment of Abaqus Explicit with the Hill (1948) plasticity model. The stress state parameters η and $\bar{\theta}$ for each test were obtained through detailed FE simulations, and the Hill (1948) equivalent strain to fracture for every test was determined by a hybrid method of DIC and FEA. A Matlab subroutine was written to minimize the Mean Squared Error (MSE) between the test results and fracture envelope and to optimize the values of C_1 , C_2 and C_3 . The calibrated MMC parameters are listed in Table 3. One can see a small MSE value for tests, which shows a strong data fitting ability of the MMC fracture envelope.

Table 3. Calibrated MMC parameters of DP steel and MSE for the calibration

Material	C_1	C_2	C_3	MSE
DP590	0.1281	536 MPa	0.9115	6.1%
DP780	0.1535	720 MPa	0.9882	5.3%
DP980	0.1693	926 MPa	1.1574	5.8%
DP1180	0.1855	1110 MPa	1.2615	7.2%

A user material subroutine (VUMAT) in the environment of Abaqus Explicit with both the Hill (1948) plasticity and MMC fracture model was implemented to simulate the present tests. The element deletion technique is used to model the fracture process and the added damage parameters caused the mesh to disappear to realize the specimen fracture. When the fracture parameter reaches 1, the specimen is damaged and fractured. Figure 4 shows fracture of the tensile test specimen at different angles, which is consistent with the test results. The comparison of the fracture curves of the 0° specimen is shown in Fig. 5a.

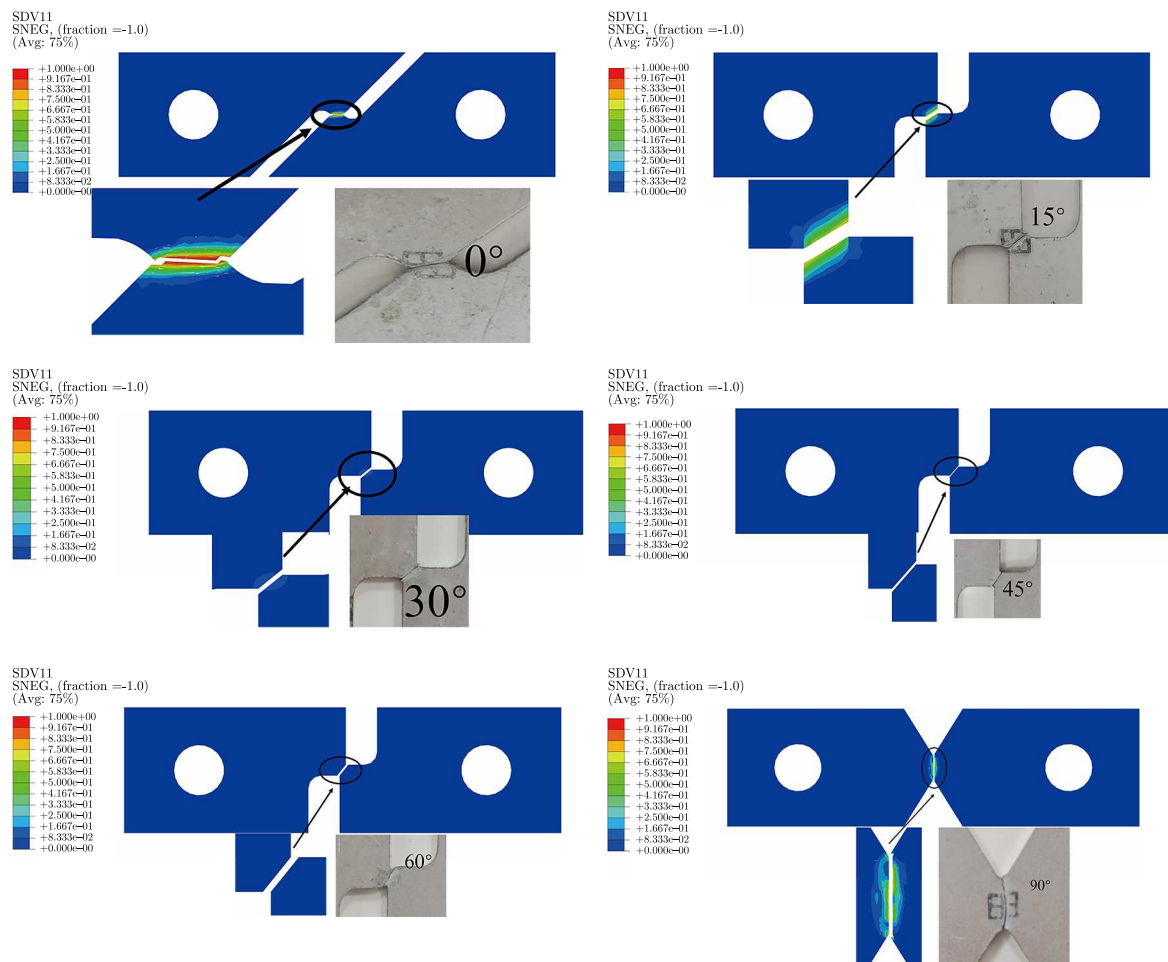


Fig. 4. Comparison of simulation fracture models

3.3. Parameter correlation

Figure 5b shows the values of three MMC parameters under different steel sheets. As the yield strength of steel sheets increases, the three parameters of MMC show an upward trend, and the interval of each parameter is relatively fixed.

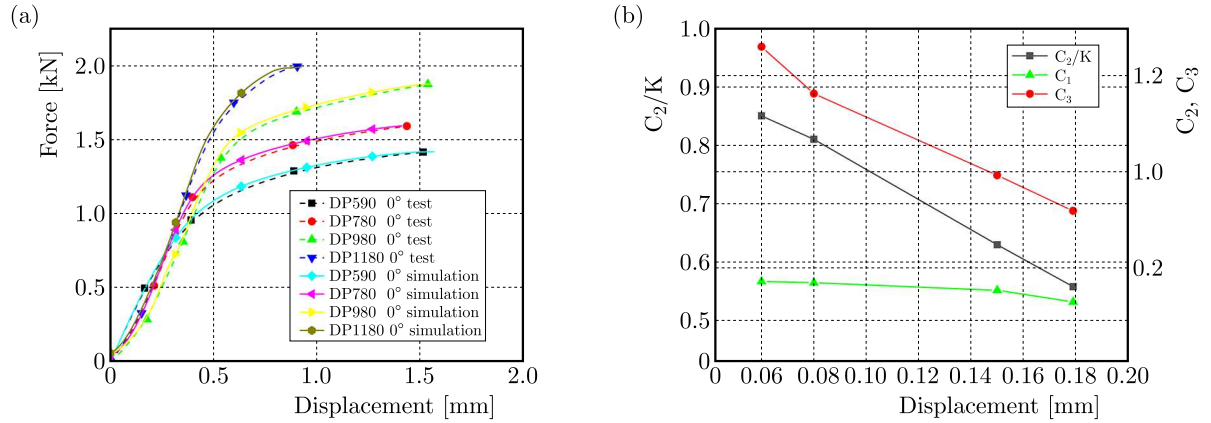


Fig. 5. (a) Comparison of load-displacement responses of simulations with 0° shear specimen against experimental data. (b) MMC parameters curve

The currently used process of solving MMC fracture parameters is relatively cumbersome and requires at least three test results to solve the equations. Therefore, it is important to study the correlation between the obtained MMC parameters and the material properties of DP steel. It is found that the C_1 range is concentrated between 0.1-0.3, the C_2 parameter is about 90% of the tensile strength, and the C_3 fluctuates around 1. The correlation between the three fracture parameters and the material properties (K, n) of DP steel is built as shown in Eq (3.3), R^2 represents goodness of fit, which is the degree to which the regression line fits the observed value. The three parameters of C_1, C_2, C_3 are respectively fitted in a linear form, and the expressions were established by the work hardening index n . The preliminary fitting parameters M_D, M_P and R^2 are shown in Table 4

$$C_{1,2,3} = M_D n + M_P \quad (3.3)$$

Table 4. MMC parameters table

MMC parameters	M_D	M_P	R^2
C_1	-0.338	0.19512	0.9562
C_2	$-2.48371K$	$1.003K$	0.9991
C_3	-2.81245	1.40876	0.9871

The approximate value of the three MMC free parameters of C_1, C_2, C_3 can be initially determined with Eq. (3.2). For a kind of dual-phase steel sheet, the three parameters of the MMC criterion can be fine-tuned after employing a test curve such as a uniaxial tensile test to obtain K, n . Equation (3.3) can reduce the difficulty of solving the three parameters of the MMC criterion.

4. MMC fracture model verification

In order to verify the fracture parameters of various steel sheets and their mutual relations and the accuracy of the MMC fracture model in different intervals when stress triaxiality is greater than zero, stretch-bending tests and numerical simulations were carried out. The stretch-bending test and Nakazima test specimens were designed. The Nakazima tests and the stretch-bending tests were carried out through a punching machine. The VUMAT fracture subroutine was embedded in Abaqus to simulate the MMC fracture under different fracture conditions.

4.1. Stretch-bending tests and simulation

4.1.1. Stretch-bending tests

The punching machine (Fig. 6a) has been used to perform stretch-bending tests on different steel samples with different rounded dies. Figure 6b shows the unbroken stretch-bending test to establish a basis for comparing the fracture simulation models. Figure 8 shows the fractured stretch-bending test. Figure 8a shows the stretch-bending specimens with tensile fracture. Figure 8b shows the change from shear fracture to tensile fracture with rounded corners and specimens. Figure 8c shows the shear fracture specimens with multiple steel sheets and multiple rounded corners.

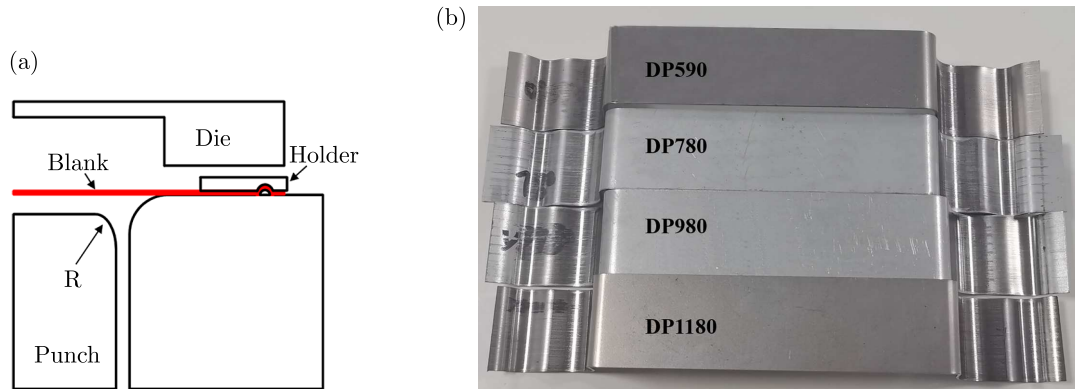


Fig. 6. (a) Punching machine mould. (b) Unbroken stretch-bending tests

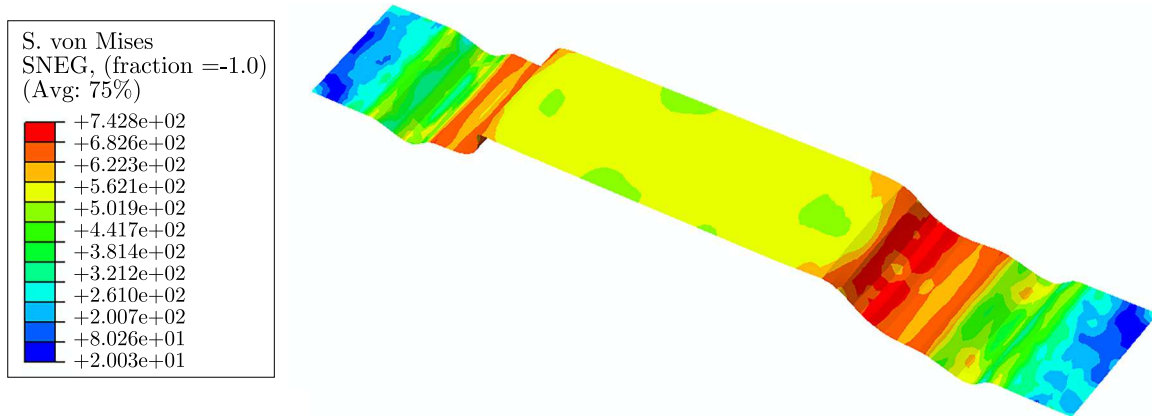


Fig. 7. Unbroken stretch-bending simulation

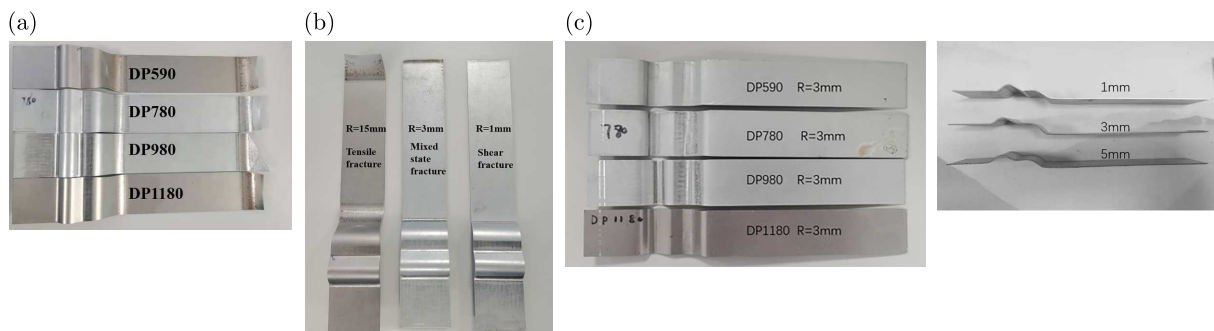


Fig. 8. Fractured stretch-bending specimens

4.1.2. Stretch-bending model verification

Establish a stretch-bending model in Abaqus and embed the VUMAT subroutine to perform a series of stretch bending simulations. As shown in Fig. 7, the stretch-bending simulation was carried out according to the blank holder force and depth in the stretch-bending test. The comparison with the test results proves that the simulation and test stretch-bending specimen results are quite good, which proves that the establishment of the MMC fractured model is relatively accurate.

4.1.3. Stretch-bending simulation verification

MMC model fracture simulation of stretch-bending specimens was carried out in ABAQUS.

To verify the accuracy of the fracture parameters of each steel sheet, based on the MMC parameters obtained in Section 3, the material properties of each steel sheet were imported into the stretch-bending model for fracture simulation. Figure 9 shows the two kinds of fracture simulation. Figure 9a shows the stretch-bending specimens with necking fracture, the stress triaxiality of necking fracture is 0.3-0.6. Figure 9b shows the stretch-bending specimens with shear fracture, the stress triaxiality ranges from 0 to 0.3. For the fractured specimens with the same fillet, compare the unbroken specimen with the unbroken simulation to verify the MMC fracture model, and verify the MMC parameters through the fractured specimen and simulation.

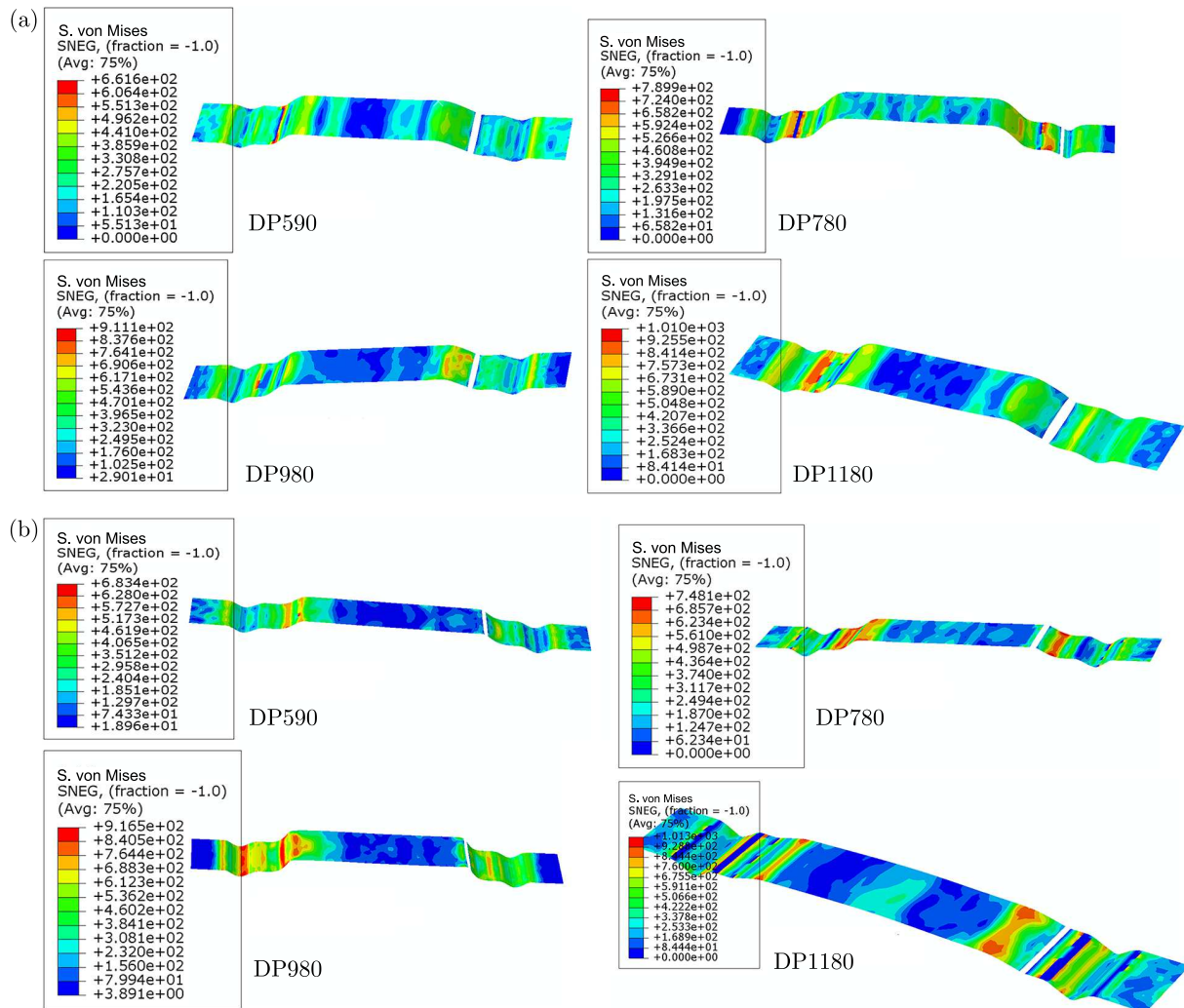


Fig. 9. Stretch-bending model fracture simulation

Compared with the test results, the fracture position of the simulation model is more consistent with the bending depth, which proves that the MMC criterion can accurately predict the necking fracture and shear fracture of DP steel sheets, and the MMC parameters are more accurate.

4.2. Nakazima tests and simulation

4.2.1. Nakazima test

In order to study the fracture condition of DP steel sheets under biaxial tension, Nakazima tests were carried out on four DP steel grades through the punching machine (Fig. 10). The circular grid was printed on the specimen through electrochemical corrosion, and the strain and fracture were determined by measuring the length of the long and short axes of the grid after fracture. The Nakazima test specimens are shown in Fig. 11.

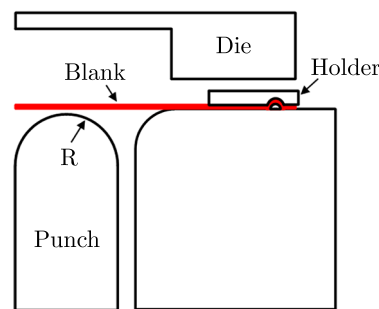


Fig. 10. Nakazima test punching machine mould

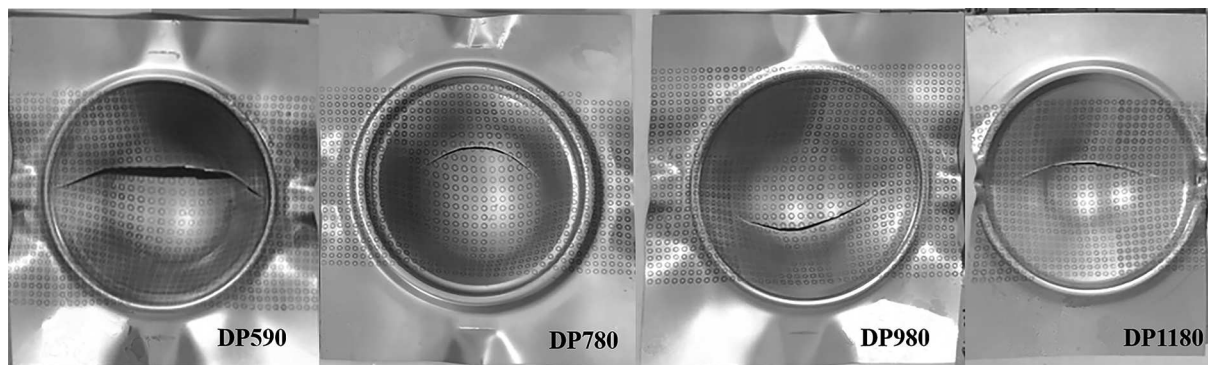


Fig. 11. Nakazima test specimens

4.2.2. Nakazima simulation verification

Establish a Nakazima model in Abaqus and embed the VUMAT subroutine to simulate the fracture under biaxial tension in a series of stretch bending simulations. The fracture condition of the MMC fracture model under biaxial tensile state was obtained by simulating the Nakazima specimens (Fig. 12), and compared with the Nakazima test, the accuracy of the MMC fracture model under the biaxial tensile state was verified. The value of stress triaxiality is 0.66. The comparison between the simulated result and the test specimen shows that the fracture location and strain are the same, which proves that the MMC fracture model can accurately predict the fracture in the biaxial tensile range, and the accuracy of MMC parameters is further verified.

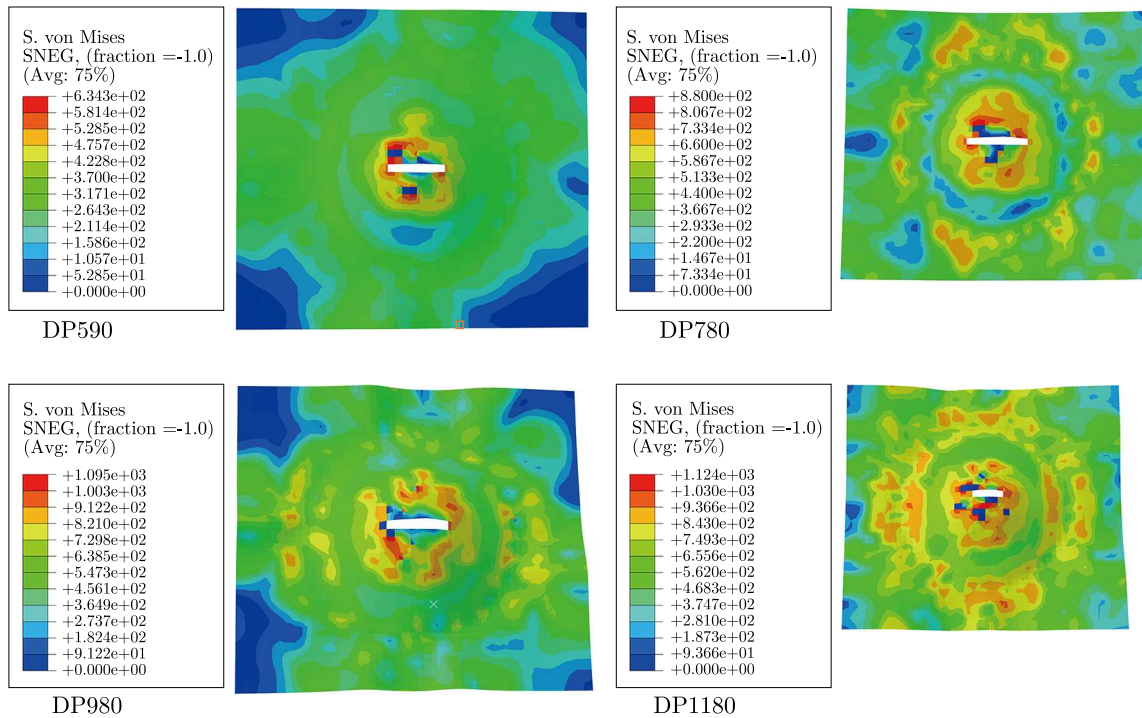


Fig. 12. Nakazima model fracture simulation

5. Conclusions

In this paper, tensile, shear and stretch-bending tests of AHSS DP steel sheets of DP590, DP780, DP980, DP1180 were designed, the equivalent strains under different stress states were obtained using the DIC-3D strain gauge, and the MMC fracture model was established to predict the tensile and shearing properties. For shear fracture, the stress triaxiality and equivalent strain were solved through a combination of more than three sets of experiments and simulations. The equations were established to obtain the MMC fracture parameters of AHSS DP steel sheets, and the model simulation parameters relationships of different steel sheets were determined. Combining the performance parameters of different AHSS DP steel sheets, the expression for MMC fracture parameters was established. Finally, the accuracy of the MMC parameters was verified through stretch-bending, Nakazima tests and simulations. The main conclusions of this research are:

- By comparing the numerical results and experimental data of the AHSS (DP590, DP780, DP980, DP1180) tensile and shear tests, it proves that the MMC simulated fracture model can also accurately predict the ductile fracture of DP980 and DP1180. It is proved by fracture simulation that the MMC fracture criterion is applicable to a wide range of stress triaxiality for the ductile fracture of DP steel.
- Based on the property parameters of the four kinds of sheet materials, MMC fracture parameter curves of the AHSS DP steel sheets DP590, DP780, DP980, DP1180 were established by fitting the correlation curves of C_1 , C_2 and C_3 with the material properties K and n . For a kind of dual-phase steel sheets, the approximate values of C_1 , C_2 and C_3 of the MMC criterion were preliminarily determined with material properties, and then the MMC criterion can be fine-tuned employing a test curve such as a uniaxial tensile test, which reduces the difficulty of solving the three parameters of the MMC criterion.

Acknowledgment

The project was supported by China-Sino Truck Group industry-university-research cooperation program project (No. 20200810).

References

1. BAI Y., WIERZBICKI T., 2010, Application of extended Mohr-Coulomb criterion to ductile fracture, *International Journal of Fracture*, **161**, 1, 1-20
2. BARLAT F., BREM J.C., YOON J.W., CHUNG K., DICK R.E., LEGE D.J., CHOI S.-H., CHU E., POURBOGHRAAT F., 2003, Plane stress yield function for aluminum alloy sheets, Part I: Theory, *International Journal of Plasticity*, **19**, 9, 1297-1319
3. DURRENBERGER L., MOLINARI A., RUSINEK A., 2008, Internal variable modeling of the high strain-rate behavior of metals with applications to multiphase steels, *Materials Science and Engineering A*, **478**, 1-2, 297-304
4. GOTOH M., KATOH M., YAMASHITA M., 1997, Studies of stretch-drawing process of sheet metals, *Journal of Materials Processing Technology*, **63**, 123-128
5. GRANUM H., MORIN D., BØRVIK T., HOPPERSTAD O.S., 2021, Calibration of the modified Mohr-Coulomb fracture model by use of localization analyses for three tempers of an AA6016 aluminium alloy, *International Journal of Mechanical Sciences*, **192**, 15, 106122
6. HILL R.A., 1948, A theory of the yielding and plastic flow of anisotropic metals, *Proceedings of the Royal Society of London*, **193**, 1033
7. JI C., LI Z., LIU J., 2020, Development of an improved MMC-based fracture criterion characterizing the anisotropic and strain rate-dependent behavior of 6061-T5 aluminum alloy, *Mechanics of Materials*, **150**, 11, 103598
8. LEE M.G., KIM D., KIM C.M., WENNER M.L., WAGONER R.B., CHUNG K., 2005, Spring-back evaluation of automotive sheets based on isotropic-kinematic hardening laws and non-quadratic anisotropic yield functions, Part II: characterization of material properties, *International Journal of Plasticity*, **21**, 883-914
9. LEVY B.S., VAN TYNE C.J., 2009, Predicting breakage on a die radius with a straight bend axis during sheet forming, *Journal of Materials Processing Technology*, **209**, 2038-2046
10. LI Y., LUO M., GERLACH J., WIERZBICKI T., 2010, Prediction of shear-induced fracture in sheet metal forming, *Journal of Materials Processing Technology*, **210**, 14, 1858-1869
11. LIAN J., SHARAF M., ARCHIE F., MÜNSTERMANN S., 2013, A hybrid approach for modelling of plasticity and failure behaviour of advanced high-strength steel sheets, *International Journal of Damage Mechanics*, **22**, 2, 188-218
12. LIAN J., WU J., MÜNSTERMANN S., 2015, Evaluation of the cold formability of high-strength low-alloy steel sheets with the modified Bai-Wierzbicki damage model, *International Journal of Damage Mechanics*, **24**, 3, 383-417
13. LOU Y., HUH H., 2013, Prediction of ductile fracture for advanced high strength steel with a new criterion: Experiments and simulation, *Journal of Materials Processing Technology*, **213**, 8, 1284-1302
14. MENG L., CHEN X., SHI M.F., SHIH H.C., 2010, Numerical analysis of AHSS fracture in a stretch-bending test, *American Institute of Physics Conference Series*, American Institute of Physics
15. QIAN L., JI W., WANG X., SUN C., MA T., 2020, Research on fracture mechanism and prediction of high-strength steel sheet under different stress states (in Chinese), *Chinese Journal of Mechanical Engineering*, **56**, 24, 72-80
16. SHIH H., 2009, An experimental study on shear fracture of advanced high strength steels, *Presentations of Great Design in Steel 2009*, Detroit, MI.
17. SHIH H.C., SHI M.F., 2008, Experimental study on shear fracture of advanced high strength steels, *Proceedings of International Conference on Manufacturing Science and Engineering*, MSEC 2008-72046
18. SRIRAM S., WONG C., HUANG M., YAN B., 2003, Stretch-bendability of advanced high strength steels, *Proceedings of SAE 2003 Word Congress*, Detroit, MI, SAE 2003-01-1151

19. WALP M.S., WURM A., SIEKIRK J.F., DESAI A.K., 2006, Shear fracture in advanced high strength steels, *Proceedings of SAE 2006 Word Congress*, Detroit, MI, SAE 2006-01-1433
20. WIERZBICKI T., BAO Y., LEE Y.-W., BAI Y., 2005, Calibration and evaluation of seven fracture models, *International Journal of Mechanical Sciences*, **47**, 4-5, 719-743
21. WIERZBICKI T., XUE L., 2005, On the effect of the third invariant of the stress deviator on ductile fracture, *Technical Report*, Impact and Crashworthiness Lab., Massachusetts Institute of Technology
22. XUE L., 2007, Damage accumulation and fracture initiation in uncracked ductile solids subject to triaxial loading, *International Journal of Solids and Structures*, **44**, 16, 5163-5181
23. XUE L., WIERZBICKI T., 2009, Numerical simulation of fracture mode transition in ductile plates, *International Journal of Solids and Structures*, **46**, 6, 1423-1435
24. YOSHIDA F., UEMORI T., FUJIWARA K., 2008, Elastic-plastic behavior of steel sheets under in-plane cyclic tension-compression at large strain, *Proceedings of Symposium on Constitutive Equations and their Role in Applied Deformation Behavior*, **18**, 633-659

Manuscript received January 12, 2022; accepted for print January 30, 2022